How to cite: *Angew. Chem. Int. Ed.* **2024**, *63*, e202401912
doi.org/10.1002/anie.202401912

Biocatalysis

Engineering a Dual-Functionalized PolyHIPE Resin for Photobiocatalytic Flow Chemistry

*Emmanouil Broumidis and Francesca Paradisi**

Abstract: The use of a dual resin for photobiocatalysis, encompassing both a photocatalyst and an immobilized enzyme, brings several challenges, including effective immobilization, maintaining photocatalyst and enzyme activity and ensuring sufficient light penetration. However, the benefits, such as integrated processes, reusability, easier product separation, and potential for scalability, can outweigh these challenges, making dual resin systems promising for efficient and sustainable photobiocatalytic applications. In this study, we employed a photosensitizer-containing porous emulsion-templated polymer as a functional support that is used to covalently anchor a chloroperoxidase from *Curvularia inaequalis* (CiVCPO). We demonstrate the versatility of this heterogeneous photobiocatalytic material, which enables the bromination of four aromatic substrates, including rutin—a natural occurring flavonol—under blue light (456 nm) irradiation and continuous flow conditions.

Introduction

Enzymes serve as efficient catalysts, promoting a plethora of transformations under eco-friendly conditions.[1] In recent years, biocatalysis is increasingly utilized both in academic and industrial settings, but enzymes that require expensive cofactors, such as nicotinamide adenine dinucleotide phosphate (NAD(P)H) or flavins, are indeed less straightforward. Alternative, cheaper artificial cofactors have been explored, although their mass synthesis presents challenges.[2] Photocatalysis, on the other hand, offers an affordable strategy for in situ cofactor generation and recycling.[3] Photosensitizers (PS) absorb light, enabling the transfer of photoexcited electrons to oxidized cofactors for regeneration. Notably, PS can also be used to generate various reactive oxygen species (ROS) like hydrogen peroxide (H_2O_2) in situ, which can serve as co-substrates to specific enzymes. An electron donor (ED) like ethylenediaminetetraacetic acid (EDTA) or methanol (MeOH) is required to complete the catalytic cycle[4] (Figure 1A).

Many water-soluble organic dyes have been used as PS for redox photobiocatalysis, including porphyrins,[5] xanthenes,[6] Ru/Ir complexes,[7] and flavins.[8] However, these PSs have limitations including problematic catalyst separation and recovery, stability concerns, scalability issues, and potential environmental impact. In contrast, heterogeneous PSs can provide better stability, reusability, and scalability, with minimal environmental impact.[9]

Existing examples of heterogeneous photobiocatalytic systems are scarce and come with their own challenges. These materials are based on Au-coated TiO_2 nanoparticles,[10,11] lignin,[12] carbon nitrides,[13] or quantum dots (QDs).[14] The first three require UV light, potentially harmful to enzymes, while quantum dots have durability and toxicity issues.

An exciting alternative to overcome the current limitations is the development of continuous flow photobiocatalytic systems with heterogeneous PS and immobilized biocatalysts in packed bed reactors (PBRs). On the one hand, photocatalysis done through flow systems provides better mass transfer, precise control, light penetration, continuous operation, increased productivity, and easier

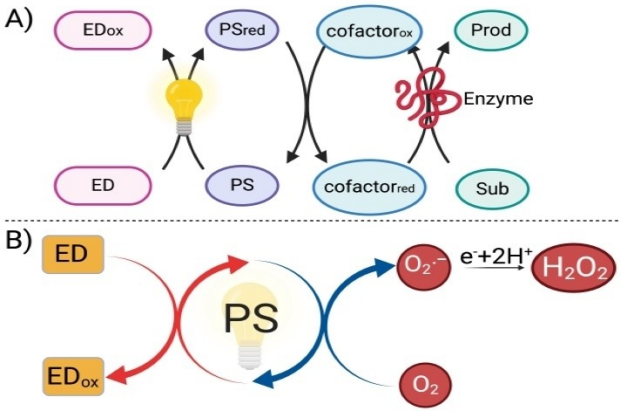

Figure 1. A) Typical photobiocatalytic transformation in which the PS is used to recycle a cofactor. B) Scheme showing production of H_2O_2 from O_2 by a PS. In the presence of an ED and light, the PS can participate in type I electron transfer from molecular oxygen to generate superoxide radicals ($O_2^{\bullet-}$).

[*] E. Broumidis, F. Paradisi
Department of Chemistry, Biochemistry and Pharmaceutical Sciences
University of Bern
Freiestrasse 3, CH3012, Bern, Switzerland
E-mail: francesca.paradisi@unibe.ch

scale-up.[9] On the other, biocatalysis in flow, with (covalently) immobilized enzymes, avoids catalyst separation issues and enzyme leaching, improves operational stability, and allows multiple reaction cycles.[15] Therefore, we postulate that this combined approach could lead to more efficient, sustainable, and cost-effective photobiocatalytic processes suitable for industrial applications.[16]

The vanadium-dependent chloroperoxidase from *Curvularia inaequalis* (CiVCPO), in the presence of H_2O_2 (co-substrate) and a halide anion (X^-), promotes the production of hypohalite species (XO^-) which can then induce electrophilic halogenation of suitable organic substrates. CiVCPO is well characterized, exceptionally robust, as it can operate in a wide range of pH values and temperatures, tolerates the use of organic solvents and retains its activity for prolonged periods of time, even at relatively high H_2O_2 concentrations (500 mM for up to 1 h).[17,18] For these reasons, we selected CiVCPO as a model enzyme for this work. We showcase herein how we designed a bifunctional photoactive material capable of supporting the CiVCPO and generating H_2O_2 in situ by a photocatalytic approach (Figure 1B), and its compatibility with flow set ups.

Results and Discussion

For the PS, we explored the viability of two types of compounds containing 2,1,3-benzothiadiazole (BTZ) and 4,4-difluoro-4-bora-3a,4a-diaza-s-indacene (BDP) moieties. These organic PS (orgPS) have been used extensively in photoredox applications and ROS production.[19,20] In most cases, both cores can be photo-excited by visible-light photons, which minimizes enzyme deactivation effects, unlike high-energy UV photons[21] that are required by many existing photobiocatalytic applications. In order to assess the photostability of CiVCPO we conducted a series of experiments where the enzyme was irradiated by six different light sources at room temperature. The enzyme, when exposed to UV light sources (370 and 390 nm) rapidly loses activity, and is catalytically inactive after 24 h and about 72 h, respectively. When violet light (427 nm) was used, CiVCPO maintained approximately 60 % activity over the first 18 h, while when the light source was >456 nm the biocatalyst was remarkably photostable even after 72 h of continuous irradiation (Figure 2).

This behavior was maintained even when the irradiation was carried out at 40 °C.

Next, we synthesized a series of homogeneous and heterogeneous BTZ and BDP orgPS materials (Figure 3; full synthetic and characterization details are provided in ESI, S1.2) and evaluated their ability to produce H_2O_2 when exposed to light (Table 1).

More specifically, for the heterogeneous materials we focused on using polymerized high internal phase emulsion (PolyHIPE) polymers, which are derived from various monomers such as styrene, and offer attractive properties like high porosity, mechanical strength and chemical resistance, making them suitable for diverse applications in areas like tissue engineering, and catalyst supports.[22] In 2017,

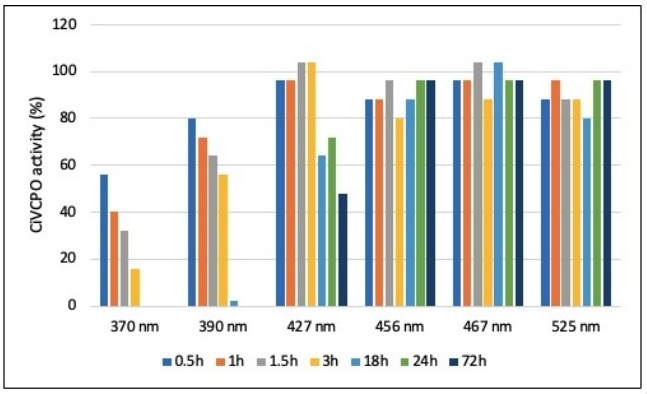

Figure 2. Photostability profile of CiVCPO enzyme. Initial protein concentration was 0.950 mg/mL (in 50 mM phosphate buffer) and specific activity 2.05 U/mg (100 %). For each test, 200 µL of protein solution was placed in a sealed HPLC glass vial. The light source was located 4 cm away from the sample. In all cases, the temperature range of the enzyme solutions was kept between 35 and 40 °C.

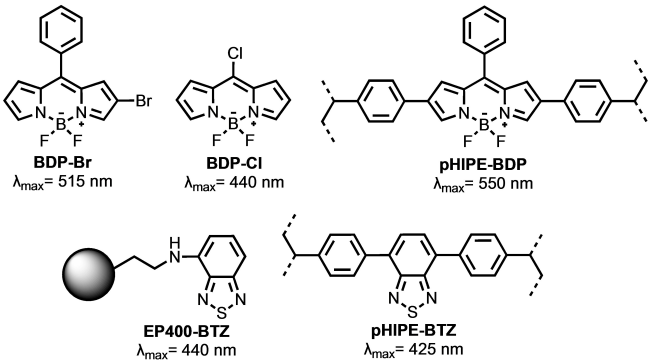

Figure 3. Series of monomeric and polymeric orgPS materials that were synthesized to test their efficacy for in situ production of H_2O_2. The maximum light absorption in the visible region for each compound is indicated as λ_{max}.

Table 1: Screening of various orgPS to determine their ability to produce H_2O_2 at various photon wavelengths.[a]

Entry	orgPS	Type	λ_{exc}	$[H_2O_2]_{max}$ (µM)
1	BDP-Cl	homogeneous	525	11
2	BDP-Cl	homogeneous	467	86
3	BDP-Br	homogeneous	525	44
4	BDP-Br	homogeneous	467	56
5[b]	pHIPE-BTZ	heterogeneous	456	64
6[c]	pHIPE-BTZ	heterogeneous	456	25
7[c]	pHIPE-BDP	heterogeneous	525	13
8[b,d]	EP400-BTZ	heterogeneous	456	3

[a] Effective concentration of orgPS in all experiments was 0.01 mM. Each orgPS was placed in a sealed vial containing a stirred solution of 10 mL 50% MeOH/Phosphate (NaPi, 50 mM) buffer (pH 6). The light source was placed 4 cm away from the vials (vial volume = 5 mL). Samples were measured 24 h after the start of the experiment. H_2O_2 concentrations were measured by the ABTS-HRP assay.[24] [b] 3 mol% orgPS loading. [c] 1 mol% orgPS loading. [d] Sample measured after 2 h, as the material had photobleached substantially at this point.

Vilela and co-workers showed that by incorporating catalytic amounts of the cross-linking unit 4,7-bis(4-vinylphenyl)benzo[*c*][1,2,5]thiadiazole (divinyl-BTZ) orgPS in the organic phase, it was possible to produce photoactive monoliths that upon illumination with blue light could access the triplet state and produce ROS, including singlet oxygen ($^1O_2$) and superoxide radical cations ($O_2^{\bullet-}$) in flow.[23] We postulated that since $O_2^{\bullet-}$ is rapidly converted to H_2O_2 in the presence of water,[20] we could use this material (pHIPE-BTZ) for our intended application.

In addition, by synthesising the monomeric BDP analogue of divinyl-BTZ, 5,5-difluoro-10-phenyl-2,8-bis(4-vinylphenyl)-5*H*-4λ^4,5λ^4-dipyrrolo[1,2-*c*:2′,1′-*f*]-[1,3,2]diazaborinine (divinyl-BDP; ESI, S1.2), we were able to create the corresponding pHIPE-BDP polymer. Incorporation of the BDP moiety in the polymeric structure was confirmed by the material UV/Vis absorption profile which features strong absorption band at around 550 nm, characteristic of BDP compounds.[25] In order to have a functional material to enable covalent enzyme immobilization, a third polymeric orgPS was also prepared, using a commercially available methacrylate resin with surface epoxide groups, EP400,[26] and 4-Amino-2,1,3-benzothiadiazole (ESI, S2.4), resulting in the EP400-BTZ material. Finally, two known soluble BDP compounds were also included in the study. These contained a halogen (Cl and Br) atom each, which could enhance their ROS production rates, by the increased intersystem crossing (K_{ISC}) due to the heavy atom effect.[27] As seen in Table 1 (entries 1–4), the homogeneous BDPs were indeed capable of generating H_2O_2 with BDP–Cl offering the highest concentrations (Table 1, entry 2). Despite their satisfactory performance however, these materials suffered from severe photobleaching within 24 h, as judged by the marked reduction in their fluorescence spectra (ESI, S2.2) making them unsuitable for prolonged use. Heterogeneous materials were tested next. pHIPE-BTZ (Table 1, entry 5) produced the highest H_2O_2 concentrations, while it retained approximately 80 % of its activity after 24 h of irradiation. In contrast, pHIPE-BDP and EP400-BTZ (Table 1, entries 7 and 8) performed very poorly; both produced low to negligible H_2O_2 concentrations, while almost completely photobleaching within 90 min of irradiation. pHIPE-BTZ was therefore selected as a photoactive support and its H_2O_2 production capability in a continuous flow set-up was investigated (Table 2).

Different solvent systems and residence times (Rt) were investigated. To our surprise, even when only water was used as the solvent without any auxiliary ED, H_2O_2 production was observed (Table 2, entry 1b), which outperformed binary solvents systems containing MeOH and DMF. This result indicates that the pHIPE-BTZ material is capable of utilising H_2O as ED.[28] Since MeOH and DMF as miscible co-solvents (Table 2, entries 2–9) provided diminished H_2O_2 outputs, we attempted to employ a biphasic system (Table 2, entries 10–12) comprising H_2O and 2-methyltetrahydrofuran (2-MeTHF), a green solvent derived from plant biomass.[29] This modification boosted H_2O_2 production by almost 100-fold as compared to the MeOH/DMF systems. We postulate that this is due to the ability of 2-MeTHF to swell the hydrophobic pHIPE/BTZ foam, leading to increased ROS production. Finally, it appeared that introducing air into the system or increasing the residence time to 30 minutes did not provide any tangible benefits.

Table 2: Parameter screening to determine optimal H_2O_2 output of pHIPE-BTZ monolith under continuous flow conditions.[a]

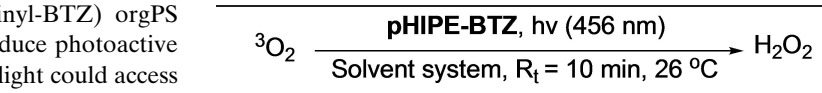

Entry	Solvent system	Rt (min)	H_2O_2 Output (μM)
1[b]	H_2O	10	18.6
2	H_2O/MeOH (9:1)	10	1.96
3	H_2O/MeOH (6:4)	10	1.00
4	H_2O/DMF (9:1)	10	7.42
5	H_2O/DMF (9:1)	10 (air)	13.6
6	H_2O/DMF (9:1)	30	7.05
7	H_2O/DMF (3:1)	10	5.60
8	H_2O/DMF (3:1)	10 (air)	9.05
9	H_2O/DMF (3:1)	30	6.0
10[c,d]	**H_2O/2-MeTHF (1:1)**	**10**	**115.7**
11	H_2O/2-MeTHF (1:1)	10 (air)	97.9
12	H_2O/2-MeTHF (1:1)	30	89.8

[a] Unless otherwise stated, the H_2O component of the solvent system contains citrate (50 mM, pH 6) buffer, which is frequently used for CiVCPO-mediated halogenations. H_2O_2 output with modifications: [b] no buffer: 17.1 μM; [c] NaPi buffer (50 mM, pH 6): 110.3 μM; [d] no buffer: 115.8 μM.

Next, we turned our attention to the immobilization of CiVCPO onto a solid support. By employing the open-source bioinformatics package CapiPy,[30] it was revealed that about 10 % of the exposed surface residues are lysines, which could therefore be exploited to covalently immobilize CiVCPO on a solid support with available epoxy or aldehyde surface groups.[31] Commercially available methacrylate resins bearing epoxy groups $EP400_{epoxy}$ and $EP403_{epoxy}$ were selected as a benchmark supports for the covalent immobilization of CiVCPO. Furthermore, through established protocols[32] we converted the epoxy surface groups to aldehydes, generating $EP400_{aldehyde}$ and $EP403_{aldehyde}$ materials. Lastly, as the EP400-BTZ failed as photoactive material, we prepared an aldehyde-functionalised version of the photoactive pHIPE-BTZ support, in order to immobilize our model enzyme directly onto it. To achieve this, we followed the same procedure that was used to obtain pHIPE-BTZ,[23] but we also included 5 mol % of 4-vinylbenzoic acid in the organic phase of the emulsion (Figure 4).

Following polymerisation, impurities were removed by Soxhlet extraction, and a bright-yellow foam was obtained. Carboxylic acid (−COOH) groups incorporation was qualitatively confirmed.[33] Treatment of the foam with *N*-ethyl-*N*′-(3-(dimethylamino-propyl)carbodiimide (EDC) and *N*-hydroxysuccinimide (NHS) afforded the corresponding NHS ester intermediate.[34] This was followed by the addition of ±-3-aminopropane-1,2-diol resulting in the introduction of a diol functionality, which was oxidised to the target aldehyde in the next step by sodium periodate ($NaIO_4$). By quantifying the consumption of $NaIO_4$ in this

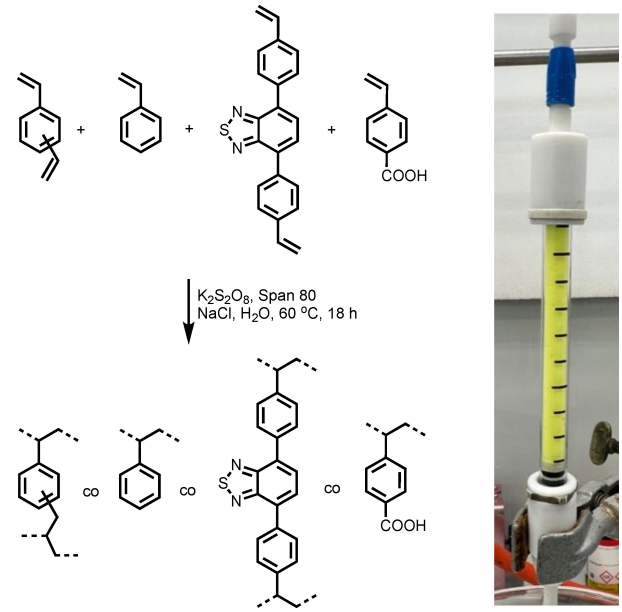

Figure 4. Synthesis of the -COOH functionalized version of the pHIPE-BTZ material. The organic phase contained styrene, divinylstyrene (DVB), divinyl-BTZ (3 mol%), and 4-vinylbenzoic acid (5 mol%). Right: Polymerized resin in column.

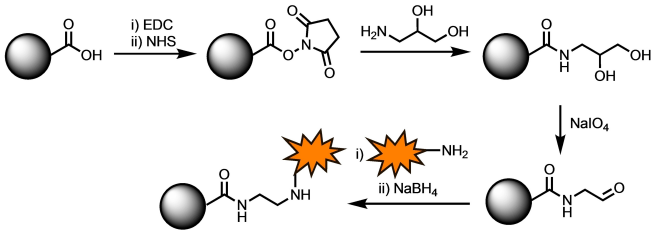

Scheme 1. Conversion of the pHIPE-BTZ_{COOH} support (gray sphere) into pHIPE-$BTZ_{aldehyde}$ and subsequent immobilization of the CiVCPO enzyme (orange 'star'). Full details about the synthetic procedures can be found in ESI, S2.

Table 3: Immobilization screening of CiVCPO on different supports.[a]

Entry	Resin	Protein loading (mg/g)	Imm. Yield (%)	Imm. activity (U/g)	Recovered activity (%)
1	EP400 epoxy	1	43	0.99	113
2	EP403 epoxy	1	31	0.51	80
3	EP400 aldehyde	1	77	1.16	73
4	EP403 aldehyde	1	75	1.26	82
5	pHIPE-BTZ aldehyde	1	100	1.30	63
6	pHIPE-BTZ aldehyde	2.5	98	1.66	82
7	pHIPE-BDP aldehyde	5	79	0.65	40

[a] Initial specific activity of CiVCPO was 2.05 U/mg, as determined by the Bradford assay.

step,[35,36] we determined to have introduced 53.4 μmol of diols/$g_{support}$, which is comparable to that of the available epoxy groups in the EP400/403 supports (ca. 70 μmol/$g_{support}$). The final step was to immobilize CiVCPO onto the resulting pHIPE-$BTZ_{aldehyde}$ support and reduce the resulting imine bond to a stable amine (Scheme 1).

To determine the efficacy of the new pHIPE-$BTZ_{aldehyde}$ support, we measured common enzyme immobilization metrics, including immobilization yield, immobilized activity and recovered activity, and compared them to those measured by using the EP400/403 resins (Table 3). The epoxy supports (Table 3, entries 1 and 2), offered modest immobilization yields and high recovered activities. With the aldehyde analogues (Table 3, entries 3 and 4), higher immobilization yields, and equivalent recovered activities were achieved. The immobilized CiVCPO showed excellent stability over three reaction cycles (ESI, S2.6). Immobilization on pHIPE-$BTZ_{aldehyde}$ foam was then carried out with three different protein concentrations (Table 3, entries 5–7). With 2.5 $mg_{protein}/g_{support}$ the immobilization yield was almost quantitative, and immobilized activity and recovered activity were maximized. However, at 5 $mg_{protein}/g_{support}$ (Table 3, entry 7) the immobilization yield decreased to 79%, indicating a saturation of the functional groups available on the material.

Analogous to the EP400/403, the enzymatic stability on pHIPE-$BTZ_{aldehyde}$ support was excellent, showing no leaching of the biocatalyst (ESI S2.6). Finally, the pHIPE-$BTZ_{aldehyde}$ foam with the immobilized CiVCPO was subjected to scanning electron microscopy (SEM; Figure 5). The resulting images confirmed the exceptional porosity of the pHIPE foam, which consists of a complex network of fibers approximately 300 nm wide, forming pores with approximately 1 μm diameter on average, resulting in a material with high surface area and light permeability, making it a promising candidate for conducting biotransformations in flow.

To investigate the performance of the photobiocatalytic foam, we opted to study the halogenation of rutin (**1a**), a therapeutic flavonoid found in many plants and fruits. Despite its promising medicinal profile, it has limited clinical use due to its poor solubility and low bioavailability.[37] Recent developments aim to improve these properties, potentially broadening its future clinical applications.[38] Introducing halogen atoms, may help alleviate some of these problems, particularly by improving the bioavailability[39,40] and providing a functional handle for further synthetic modifications. A packed bed reactor (PBR) was loaded with 100 mg of the photobiocatalytic resin, and a 0.1 mM solution of rutin in citrate buffer was flown through the reactor with a 10 min residence time (Scheme 2, conditions A), either as a single pass or with a recycling set-up (Figure 6). To be noted that in this reaction set up, while rutin concentration was limited by the low solubility of the substrate (it is completely insoluble in 2-MeTHF, therefore citrate buffer was selected), the limiting reagent is the H_2O_2 generated by the resin upon irradiation (Table 2, entry 1).

The reaction started when the light source (456 nm) was turned on, and HPLC monitoring (ESI, S2.8) showed the

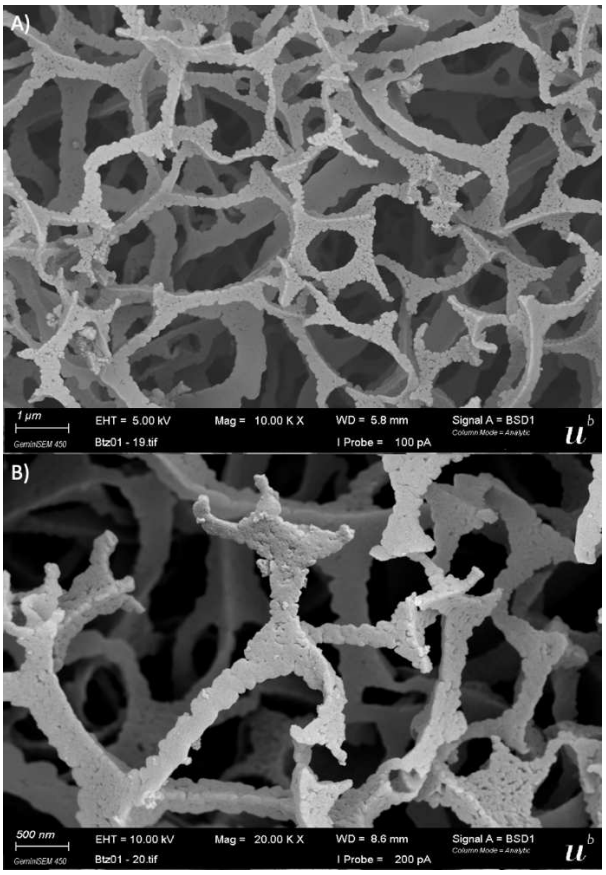

Figure 5. SEM images showing the filamentous structure of the pHIPE foam material. A) 10 k magnification, B) 20 k magnification.

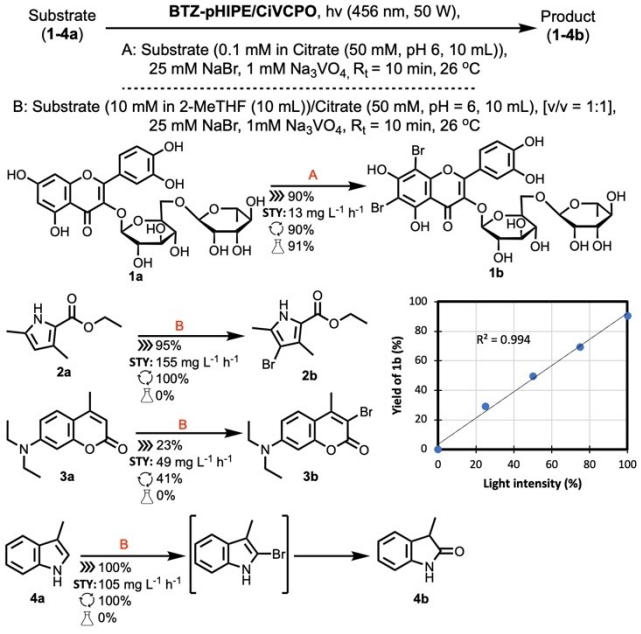

Scheme 2. Photobiocatalytic transformations carried out by the BTZ-pHIPE/CiVCPO resin under continuous flow conditions. Reaction conditions (A and B) employed for the photobiocatalytic halogenations in flow are shown under the first arrow and in red above each subsequent transformation. The single pass (⋙) product (HPLC) yield (%), STY (mg L^{-1} h^{-1}), recycling set-up (♲) yield (based on product obtained in 10 mL of solution after 48 h of irradiation), and batch (⚗) yield (10 min reaction time), are shown for each transformation. The light source was placed 4 cm away from the PBR. The temperature was kept constant at 26 °C for the duration of the reaction. PBR volume was 1.2 mL, flow rate 0.12 mL/min, residence time 10 min. Insert shows the linear relationship between light intensity and conversion into product **1b** from **1a**, as measured by HPLC.

formation of only a single product. Mass spectrometry (MS) revealed that the product had mass consistent with that of the dibrominated derivative, and no monobrominated derivative was detected. Upon further analysis the compound was identified as the dibrominated analogue 6,8-dibromorutin (**1b**; Scheme 2 and ESI, 2.7). After a single pass the conversion of **1a** to **1b** was 8.4 % (Scheme 2) which is equivalent to 90 % consumption of the available H_2O_2. With this set up, 0.1 mM rutin concentration corresponds to a space-time yield (STY) of 13 mg×L^{-1}×h^{-1}. As seen in Scheme 2 (insert), there is a linear correlation between the light output and the product yield, while no reaction occurs in the absence of illumination. In a control experiment, 100 % illumination intensity and pHIPE-BTZ without immobilized CiVCPO, no product at all was formed. These results demonstrate that the reaction is truly photobiocatalytic, requiring both light and enzyme to occur. To increase productivity, the flow set-up was switched to a recycling mode, as seen in Figure 6, and 10 mL of 0.1 mM of rutin (**1a**) was recirculated. After 48 h, just 9 % of the original activity of the resin remained, as indicated by the H_2O_2 output that was measured (ca. 10 µM) using the HRP assay as mentioned before. We postulate this was due to the presence of other ROS generated during illumination, that could photobleach the orgPS. Moreover, presence of ROS could also degrade the immobilized enzyme. Despite the

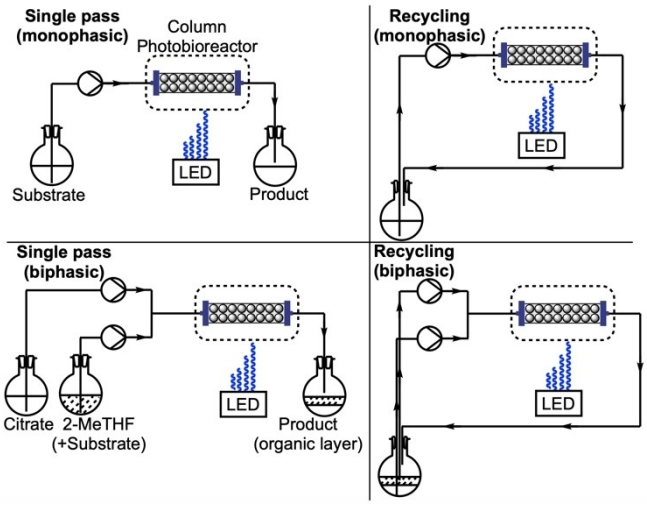

Figure 6. Modes of flow that were used for the photobiocatalytic experiments and their respective set-ups.

progressive photobiocatalyst inactivation, after 48 h of recirculation, product **1b** was produced, in 90 % yield. Two additional recirculation reactions were carried out, each

with fresh photobiocatalyst resin yielded sufficient product to be purified and isolated by semi-preparatory HPLC (ESI, S1.7).

Interestingly, even when the bromide concentration was lowered to 0.5 eq. with respect to **1a** only the dibrominated product could be observed, albeit in a lower yield. Conversely, when chlorination was attempted, no reaction occurred, which can be rationalized by the reduced activity of CiVCPO towards chlorinations.[41]

The utility of the photobiocatalytic resin was further validated in the halogenation of three additional substrates (Scheme 2, **2a**, **3a**, **4a**). For this set of reactions, we switched to a biphasic system (2-MeTHF/Citrate) similar to the one used during the H_2O_2 production studies, which was shown to be the best performer (Table 2, entry 10). In addition, by using 2-MeTHF as the organic phase, the solubility of these substrates could be increased to 10 mM. Consequently, the STY was substantially improved for all three substrates compared to rutin (**1a**); from 13, to 155, 49 and 105 $mg \times L^{-1} \times h^{-1}$ for **2a**, **3a** and **4a** respectively. Similarly to 1b, compounds **2b**, **3b** and **4b** were all isolated by switching to a recirculation set-up (48 h illumination) and were fully characterized. Notably, when halogenating 3-methylindole **4a**, instead of the 2-bromo-3-methyl-1*H*-indole, 3-methylindolin-2-one (**4b**) was obtained, due to the unstable nature of the former in acidic environments.[42] During this set of experiments, each photobiocatalytic column retained activity for at least 48 h of constant use, before the orgPS was fully degraded due to photobleaching effects. Notwithstanding this boost in performance of the biphasic system, STY′s remained comparatively low. We postulate that this limitation stems primarily from the resin's ability to generate H_2O_2, as the maximum amount measured was 115.7 μM (Table 2, entry 10), thus acting as a bottleneck when performance is concerned. Despite this, we were delighted to see that the single pass yield for substrates **1b**, **2b**, and **4b** were excellent (>90 %). The outlier, brominated coumarin derivative **3b** performed substantially worse (23 % single pass yield), which may be due to its ability to absorb light at wavelengths that overlap with the LED source (456 nm) that was used, thus limiting its efficacy.

To offer a fair comparison, we also conducted further experiments with CiVCPO under standard batch conditions. The reactions were performed in round bottom flasks and the reaction mixture had a volume of 1.2 mL, identical to the PBR in the flow experiments, and the reactions were terminated after 10 minutes to mirror the flow setup's residence time. H_2O_2 was added from a stock commercial solution at the same concentration as measured in the flow setup (conditions A: 18.6 μM and conditions B: 115.7 μM) maintaining the temperature at 26 °C, and stirring at 350 rpm. To initiate the reaction, free CiVCPO was added so that the same specific activity was achieved (0.166 U).

The results revealed a significant advantage of flow over batch conditions for the three substrates requiring a biphasic set up (B), where no product formation was observed in batch, even with an equimolar amount (10 mM) of H_2O_2. Likely the reduced mixing efficiency of the two phases in a batch reactor, despite magnetic stirring, limits mass transfer. For rutin (method A, monophasic), the batch reaction yielded equivalent results to flow with a 91 % yield, based on H_2O_2 consumption, after 10 min.

The flow approach is in all cases advantageous as the enzyme and photosensitizer are immobilized on foam, allowing for easy reuse and eliminating the need for additional purification to remove catalysts. Moreover, it facilitates the halogenation of low water-soluble compounds, which is unachievable with standard batch processing.

Conclusions

To our knowledge, this is the first example of a continuous flow biotransformation enabled by a photobiocatalytic resin, and we envisage that it will encourage others to develop and explore similar systems. However, for this synergistic approach to become truly applicable in practice, several improvements need to be made, including the use of orgPSs that can exclusively generate the desired ROS (in this case $O_2^{\bullet-}$)[43] to minimize enzymatic deactivation by other ROS. Another alternative that is worth exploring is to utilize this technology for activating redox enzymes by generating photoinduced electrons under an inert atmosphere, which should avoid the generation of ROS altogether, expanding the useful lifetime of these types of resins. Work is currently underway to develop such systems.

Supporting Information

The authors have cited additional references within the Supporting Information.

Acknowledgements

We thank Prof. Frank Hollmann for providing the CiVCPO plasmid and for useful scientific discussions. E.B. thanks the Swiss Federal Commission for Scholarships for Foreign Students (FCS) for funding (Award No: 2022.0224). We thank Dr. David Roura Padrosa at InSEIT AG for useful discussions and guidance on the immobilization of CiVCPO enzyme. Open Access funding provided by Universität Bern.

Conflict of Interest

The authors declare no conflict of interest.

Data Availability Statement

The data that support the findings of this study are available in the supplementary material of this article.

Keywords: continuous flow · photobiocatalysis · rutin · chloroperoxidase · photosensitizers

[1] E. L. Bell, W. Finnigan, S. P. France, A. P. Green, M. A. Hayes, L. J. Hepworth, S. L. Lovelock, H. Niikura, S. Osuna, E. Romero, K. S. Ryan, N. J. Turner, S. L. Flitsch, *Nat. Rev. Methods Primers* **2021**, *1*, 46.

[2] C. J. Seel, T. Gulder, *ChemBioChem* **2019**, *20*, 1871–1897.

[3] Y. Peng, Z. Chen, J. Xu, Q. Wu, *Org. Process Res. Dev.* **2022**, *26*, 1900–1913.

[4] W. Harrison, X. Huang, H. Zhao, *Acc. Chem. Res.* **2022**, *55*, 1087–1096.

[5] T. Lazarides, I. V. Sazanovich, A. J. Simaan, M. C. Kafentzi, M. Delor, Y. Mekmouche, B. Faure, M. Réglier, J. A. Weinstein, A. G. Coutsolelos, T. Tron, *J. Am. Chem. Soc.* **2013**, *135*, 3095–3103.

[6] S. H. Lee, D. S. Choi, M. Pesic, Y. W. Lee, C. E. Paul, F. Hollmann, C. B. Park, *Angew. Chem. Int. Ed.* **2017**, *56*, 8681–8685.

[7] M. R. Schreier, B. Pfund, D. M. Steffen, O. S. Wenger, *Inorg. Chem.* **2023**, *62*, 7636–7643.

[8] X. Gao, J. R. Turek-Herman, Y. J. Choi, R. D. Cohen, T. K. Hyster, *J. Am. Chem. Soc.* **2021**, *143*, 19643–19647.

[9] C. G. Thomson, A.-L. Lee, F. Vilela, *Beilstein J. Org. Chem.* **2020**, *16*, 1495–1549.

[10] W. Zhang, B. O. Burek, E. Fernández-Fueyo, M. Alcalde, J. Z. Bloh, F. Hollmann, *Angew. Chem. Int. Ed.* **2017**, *56*, 15451–15455.

[11] C. J. Seel, A. Králík, M. Hacker, A. Frank, B. König, T. Gulder, *ChemCatChem* **2018**, *10*, 3960–3963.

[12] J. Kim, T. V. T. Nguyen, Y. H. Kim, F. Hollmann, C. B. Park, *Nat. Synth.* **2022**, *1*, 217–226.

[13] M. M. C. H. van Schie, W. Zhang, F. Tieves, D. S. Choi, C. B. Park, B. O. Burek, J. Z. Bloh, I. W. C. E. Arends, C. E. Paul, M. Alcalde, F. Hollmann, *ACS Catal.* **2019**, *9*, 7409–7417.

[14] D. H. Nam, S. H. Lee, C. B. Park, *Small* **2010**, *6*, 922–926.

[15] M. Romero-Fernández, F. Paradisi, *Curr. Opin. Chem. Biol.* **2020**, *55*, 1–8.

[16] S. N. Chanquia, A. Valotta, H. Gruber-Woelfler, S. Kara, *Front. Catal.* **2022**, *1*, 816538.

[17] G. T. Höfler, A. But, F. Hollmann, *Org. Biomol. Chem.* **2019**, *17*, 9267–9274.

[18] R. Renirie, C. Pierlot, J.-M. Aubry, A. F. Hartog, H. E. Schoemaker, P. L. Alsters, R. Wever, *Adv. Synth. Catal.* **2003**, *345*, 849–858.

[19] S. Wang, B. Cai, H. Tian, *Angew. Chem. Int. Ed.* **2022**, *61*, e202202733.

[20] X. Guo, X. Li, X.-C. Liu, P. Li, Z. Yao, J. Li, W. Zhang, J.-P. Zhang, D. Xue, R. Cao, *Chem. Commun.* **2018**, *54*, 845–848.

[21] A. Lante, F. Tinello, G. Lomolino, *Innovative Food Sci. Emerging Technol.* **2013**, *17*, 130–134.

[22] A. S. Hayward, N. Sano, S. A. Przyborski, N. R. Cameron, *Macromol. Rapid Commun.* **2013**, *34*, 1844–1849.

[23] J. M. Tobin, T. J. D. McCabe, A. W. Prentice, S. Holzer, G. O. Lloyd, M. J. Paterson, V. Arrighi, P. A. G. Cormack, F. Vilela, *ACS Catal.* **2017**, *7*, 4602–4612.

[24] M. Wang, D. Wang, S. Qiu, J. Xiao, H. Cai, J. Zou, *Environ. Sci. Pollut. Res. Int.* **2019**, *26*, 27063–27072.

[25] V. Leen, P. Yuan, L. Wang, N. Boens, W. Dehaen, *Org. Lett.* **2012**, *14*, 6150–6153.

[26] D. Roura Padrosa, H. Lehmann, R. Snajdrova, F. Paradisi, *Front. Catal.* **2023**, *3*, 1147205.

[27] Y. Xiang, Y. Zhao, N. Xu, S. Gong, F. Ni, K. Wu, J. Luo, G. Xie, Z.-H. Lu, C. Yang, *J. Mater. Chem. C* **2017**, *5*, 12204–12210.

[28] M. Mifsud, S. Gargiulo, S. Iborra, I. W. C. E. Arends, F. Hollmann, A. Corma, *Nat. Commun.* **2014**, *5*, 3145.

[29] C. J. Clarke, W.-C. Tu, O. Levers, A. Bröhl, J. P. Hallett, *Chem. Rev.* **2018**, *118*, 747–800.

[30] D. Roura Padrosa, V. Marchini, F. Paradisi, *Bioinformatics* **2021**, *37*, 2761–2762.

[31] M. Romero-Fernández, F. Paradisi, in *Catalyst Immobilization* **2020**, pp. 409–435.

[32] M. Romero-Fernandez, F. Paradisi, *Green Chem.* **2021**, *23*, 4594–4603.

[33] S. Rödiger, M. Ruhland, C. Schmidt, C. Schröder, K. Grossmann, A. Böhm, J. Nitschke, I. Berger, I. Schimke, P. Schierack, *Anal. Chem.* **2011**, *83*, 3379–3385.

[34] C. Wang, Q. Yan, H.-B. Liu, X.-H. Zhou, S.-J. Xiao, *Langmuir* **2011**, *27*, 12058–12068.

[35] J. M. Guisán, *Enzyme Microb. Technol.* **1988**, *10*, 375–382.

[36] A. I. Benítez-Mateos, S. Bertella, J. Behaghel de Bueren, J. S. Luterbacher, F. Paradisi, *ChemSusChem* **2021**, *14*, 3198–3207.

[37] R. Semwal, S. K. Joshi, R. B. Semwal, D. K. Semwal, *Phytochem. Lett.* **2021**, *46*, 119–128.

[38] A. Ganeshpurkar, A. K. Saluja, *Saudi Pharm. J.* **2017**, *25*, 149–164.

[39] N. Molchanova, J. E. Nielsen, K. B. Sørensen, B. K. Prabhala, P. R. Hansen, R. Lund, A. E. Barron, H. Jenssen, *Sci. Rep.* **2020**, *10*, 14805.

[40] D. Chiodi, Y. Ishihara, *J. Med. Chem.* **2023**, *66*, 5305–5331.

[41] T. Hering, B. Mühldorf, R. Wolf, B. König, *Angew. Chem. Int. Ed.* **2016**, *55*, 5342–5345.

[42] R. L. Hinman, C. P. Bauman, *J. Org. Chem.* **1964**, *29*, 1206–1215.

[43] K.-X. Teng, W.-K. Chen, L.-Y. Niu, W.-H. Fang, G. Cui, Q.-Z. Yang, *Angew. Chem. Int. Ed.* **2021**, *60*, 19912–19920.

Manuscript received: January 27, 2024
Accepted manuscript online: March 20, 2024
Version of record online: April 17, 2024